Journal of Solid State Chemistry 183 (2010) 1900–1904

Contents lists available at ScienceDirect

Journal of Solid State Chemistry

journal homepage: www.elsevier.com/locate/jssc

Chemical synthesis of mesoporous CuO from a single precursor: Structural, optical and electrical properties

Swarup Kumar Maji [a], Nillohit Mukherjee [a,*], Anup Mondal [a,*], Bibhutosh Adhikary [a,*], Basudeb Karmakar [b,*]

[a] Department of Chemistry, Bengal Engineering and Science University, Shibpur, Howrah 711 103, West Bengal, India
[b] Glass Division, Central Glass and Ceramic Research Institute, Kolkata 700 032, West Bengal, India

ARTICLE INFO

Article history:
Received 7 April 2010
Received in revised form
8 June 2010
Accepted 13 June 2010
Available online 23 June 2010

Keywords:
Chemical route
Single precursor
Mesoporous
Nanocrystals
Photoluminescent

ABSTRACT

We report a simple method for growing photoluminescent mesoporous CuO nanoparticles by a chemical route, using the single precursor technique. The final products were characterized by powder X-ray diffraction (XRD), field emission scanning electron microscopy (FESEM), N_2 adsorption–desorption isotherm, UV–vis absorption spectroscopy, photoluminescence (PL) spectroscopy, Raman spectroscopy, Fourier transform infrared (FTIR) spectroscopy and Hall measurements. Structural analysis reveals that the average pore diameter of the as-prepared CuO is about 38.8 Å and it comes with an average surface area of 66.63 m^2/g. N_2-sorption analysis shows that the resulting isotherm as type IV; which is the characteristic of mesoporous materials. The average crystal diameter, as derived from the XRD data analysis is found to be about 20 nm. FESEM measurement reveals that the material is composed of cubic nanoparticles. The UV–vis spectrum of the material shows significant amount of blue-shift in the band gap energy (E_g), due to the quantum confinement effect exerted by the nanocrystals. The Raman study of the CuO nanostructures also indicates the high crystalline nature of the material. From the positive sign of Hall coefficient, the p-type conduction nature of the deposited film is established. The film was found to show high magnetoresistance, which is in the order of 10^5 Ω.
© 2010 Elsevier Inc. All rights reserved.

1. Introduction

CuO is a narrow band gap (E_g=1.2 eV) p-type semiconducting material with few promising applications in current days science and technology, due to its unique features like high specific surface area, chemical stability, electrochemical activity, high electron communication features, etc. It has been widely used for diverse applications such as heterogeneous catalysts [1,2], gas sensors [3,4], lithium ion electrode materials [5], high T_c superconductors [6] and field emission (FE) emitters [7–9]. It is also a promising material for fabricating solar cell, due to its photoconductive and photochemical properties [10,11]. Recently, CuO nanomaterials have also been synthesized in 2D and 3D structures by other groups [12]. Although great progresses have been made in the synthesis of CuO nanoparticles; hierarchical CuO architectures composed of nanoscale building blocks are seldom reported. Therefore, the synthesis and fabrication of CuO nanomaterials have both fundamental and practical importance.

In this work, we report a simple and single precursor approach for the synthesis of cubic shaped mesoporous CuO nanostructures. The final products were characterized by powder XRD, FESEM, FTIR, UV–vis absorption spectroscopy, photoluminescence (PL) spectroscopy, N_2 adsorption–desorption isotherm, thermogravimetric analysis and Hall measurement.

2. Experimental section

2.1. Synthesis of precursor $[Cu(OOCPh)_2Lut_2]$ complex

$CuCO_3$,$Cu(OH)_2$,H_2O (Qualigens), 2,6-dimethylpyridine (Lutidine) (Aldrich, 98+%), benzoic acid (Merck, 99%) and toluene (Rankem, 99.0%) used in this work were of analytical reagent (AR) grade and were used as received without further purification.

$CuCO_3$,$Cu(OH)_2$,H_2O (358 mg, 1.5 mmol), 2,6-lutidine (321 mg, 3 mmol) and 20 ml of toluene were mixed in a round-bottomed flask. Benzoic acid (366 mg, 3 mmol) dissolved in 2 ml of toluene was added drop wise and was stirred on a magnetic stirrer for 4 h at room temperature. Initially, the entire solution was pale green in color, which turned in to deep green suspension after the completion of stirring. The green colored residue was filtered and dissolved with acetonitrile and filtered again. The filtrate was kept for slow evaporation in air. After over night, a bluish green

* Corresponding authors. Fax: +91 3326682916
E-mail address: nilsci@yahoo.co.uk (N. Mukherjee).

0022-4596/$ - see front matter © 2010 Elsevier Inc. All rights reserved.
doi:10.1016/j.jssc.2010.06.007

crystalline compound was collected by filtration. Yield: ~580 mg (74.5% of yield based on cupric carbonate).

2.2. Synthesis of CuO from precursor complex

The precursor complex $Cu(OOCPh)_2Lut_2$ (520.08 mg, 1 mmol) was taken in a molybdenum boat and heated at 450 °C for 30 min in air using a quartz-tube furnace. After annealing, the precursor yielded about 79.39 mg of CuO. To prepare thin film of CuO, a saturated solution of metal precursor in acetonitrile was made and about 2 drops of the solution were taken over a cleaned glass substrate of area 2.5 cm × 1 cm, which was then dried in air for about 15–20 min; followed by annealing for 10 min at 450 °C in a quartz-tube furnace in air. The furnace was set at this temperature because $Cu(OOCPh)_2Lut_2$ complex was found to decompose to CuO at this temperature, as was observed by the thermogravimetric analysis. The procedure of deposition and annealing were repeated for 8–10 times to obtain a film with significant thickness.

2.3. Physical measurements

CHN elemental analysis was done using Perkin-Elmer 2400II CN analyzer. The composition and crystalline structure of the final product was obtained by X-ray diffraction (XRD) technique using X'pert Pro MPD diffractometer (PANalytical, Almelo, The Netherlands) operating at 40 kV–30 mA, using Ni-filtered CuK_α X-radiation (λ=1.540598 Å) with X'celerator step size 2θ=0.05°, step time 0.5 s, from 2θ=20–80°. The surface morphology of the deposited materials was studied by field emission scanning electron microscope (FESEM) using the Gemini Zeiss Supra™ 35VP model (Carl Zeiss Microimaging GmbH, Berlin, Germany) with 4.9 kV accelerating voltage. UV–vis absorption spectrum was recorded on JASCO V-530 UV–vis spectrometer. Fourier transform infrared (FTIR) spectrum was taken on a JASCO FTIR-460 Plus spectrometer. Thermogravimetric analysis (TGA) was examined by a Perkin-Elmer USA Diamond-200. The TGA experiment was carried out by heating the sample from 25 to 600 °C at a rate of 10 °C/min under dinitrogen purge. Nitrogen adsorption–desorption isotherm was obtained using a Quantachrome Instruments adsorption analyzer at 77 K. Prior to gas adsorption, sample was degassed for 1 h at 393 K. Hall measurement was carried out using an Ecopia Hall Effect Measurement System (HMS 3000) setup.

3. Results and discussion

The precursor complex was synthesized by the reaction of cupric carbonate with 2,6-lutidine and benzoic acid in a ratio of 1:2:2, toluene used as the solvent. The metal precursor complex was decomposed on annealing at 450 °C to form CuO nanocrystals. The chemical reactions that may be involved in this process can be described as

$$CuCO_3,Cu(OH)_2,H_2O + 2,6\text{-Lut} + PhCOOH \rightarrow Cu(OOCPh)_2Lut_2$$

$$Cu(OOCPh)_2Lut_2 \xrightarrow{\Delta} CuO + \text{bi-products}$$

The precursor complex was characterized by CHN elemental analysis and FTIR spectroscopy. The C, N, and H elemental analyses of the precursor complex agree with the calculated value for the proposed empirical formula within the experimental error (Calcd: C, 64.62; H, 5.42; N, 5.38. Found: C, 64.6; H, 5.47; N, 5.36). The IR spectrum of the precursor complex exhibits several diagnostic features. The ν(C=N) vibrations in the compound were observed at 1630 cm^{-1}. The complex also shows two strong bands at about 1571 and 1404 cm^{-1} in their infrared spectra, which are attributable to carboxylate ν_{as} CO_2^- and ν_s CO_2^- vibrations, respectively, and their separation by 167 cm^{-1} is consistent with the bidentate mode of binding [13]. Similar observation has also been found in the Copper (II)-complex $[Cu(PIM)_2(PhCOO)_2]$ by Peng et al. [14], where the separation of ν_{as} CO_2^- and ν_s CO_2^- vibrations is about 154 cm^{-1}. The electronic spectrum of the $Cu(OOCPh)_2Lut_2$ complex shows a d–d band at 695 nm, which is also similar to the spectrum of $Cu(PIM)_2(PhCOO)_2$ complex as obtained by Peng et al. [14]. Therefore, from UV–vis and IR spectra, octahedral geometry is suggested for the precursor and the probable structure is as shown in Fig. 1.

3.1. Thermogravimetric analysis

The curve of thermogravimetric analysis of the $Cu(OOCPh)_2Lut_2$ precursor is shown in Fig. 2. The curve showed three pronounced weight loss steps. The first weight loss (20.75%) between 70 and 160 °C was due to the decomposition of one lutidine group (calc. wt%=20.56), where the suggested product is the $Cu(OOCPh)_2Lut$. The second weight loss was observed in the temperature range 160–345 °C. In this temperature range, $Cu(OOCPh)_2Lut$ was decomposed to CuO(Lut) by the elimination of $O(OCPh)_2$ group with calculated and measured weight losses of 43.45% and 39.803%, respectively. The third weight loss was observed in the temperature range between 340 and 450 °C, where the remaining lutidine group was decomposed with calculated and measured weight losses of 20.56% and 20.909%, respectively. The possible chemical reactions for the thermal decomposition of $Cu(OOCPh)_2Lut_2$ are presented below:

$$Cu(OOCPh)_2Lut_2 \rightarrow Cu(OOCPh)_2Lut + Lut \quad (1)$$

$$Cu(OOCPh)_2Lut \rightarrow CuO(Lut) + O(OCPh)_2 \quad (2)$$

$$CuO(Lut) \rightarrow CuO + Lut\ldots \quad (3)$$

Therefore, TGA result indicates that decomposition of the precursor complex began at above ~70 °C, given 18.5% residue at ~450 °C, resulted in the formation of metal oxide. This fact is also supported by the powder X-ray diffraction pattern of the residue obtained from the TGA pan. The percentage of weight loss calculated for the CuO residue is 15.3%, which is in good agreement with the value given by TGA.

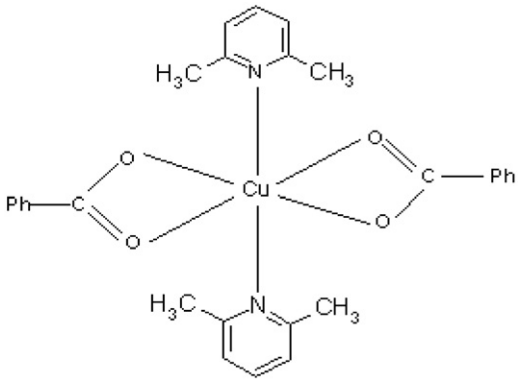

Fig. 1. Probable structure of the $Cu(OOCPh)_2Lut_2$ complex.

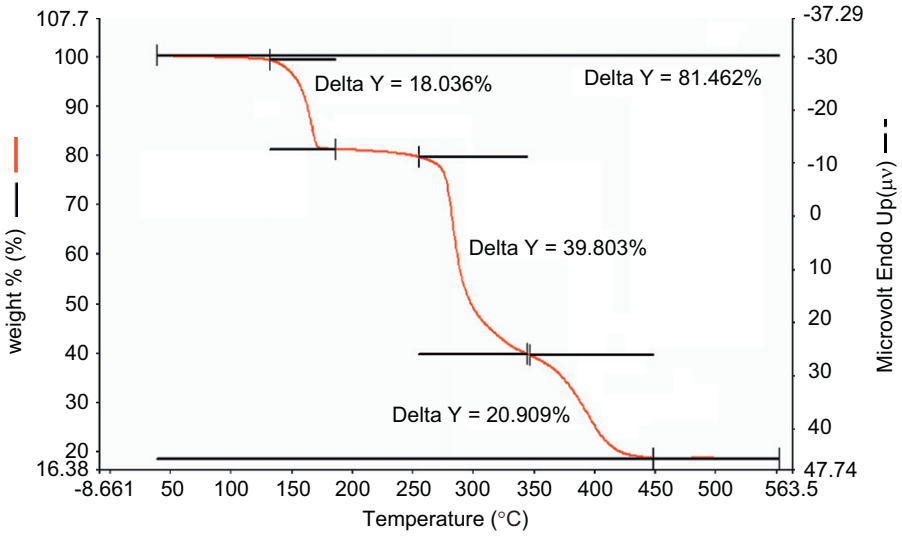

Fig. 2. TGA curve of the $Cu(OOCPh)_2Lut_2$ complex.

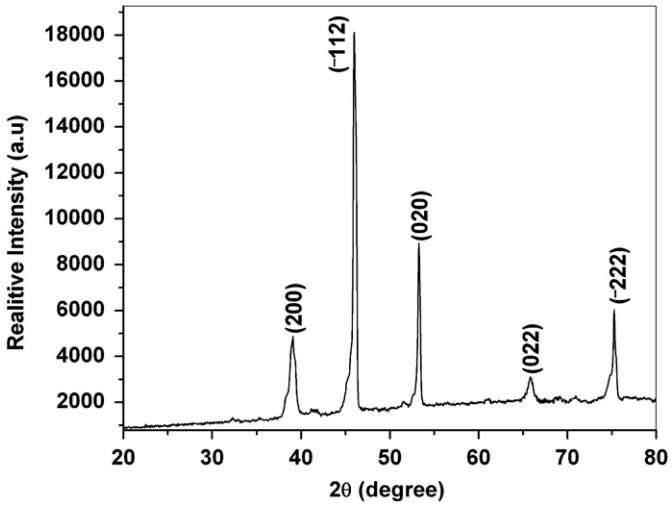

Fig. 3. X-ray diffraction pattern of CuO.

3.2. X-ray diffraction analysis

In Fig. 3, a typical XRD pattern of the CuO sample is displayed. All the peaks can be clearly indexed as tenorite CuO (JCPDS ID. 41-0254) with four major diffractions from (200) (−112), (020) and (222) planes with lattice constants $a=4.685$ Å, $b=3.423$ Å, $c=5.132$ Å and $\beta=99.52$. The values of lattice constant and β are in good agreement with the standard values for tenorite (JCPDS ID. 41-0254). The broadening of the major peaks indicates the formation of nanometric particle size, in this case, which was found to be about 20 nm (as calculated using the Scherrer equation). No diffractions from any other materials as impurity were detected, suggesting the purity of the deposited material. The value of micro-strain (ε) generated in the crystallite during the deposition process was calculated using the standard equation $\varepsilon=(\beta\cos\theta)/4$ (here, β is the value of the full-width at half-maximum for the highest intense peak) and found to be 1.7×10^{-3}.

3.3. N_2-sorption studies

The N_2 adsorption–desorption isotherm and the corresponding pore size distribution of the powder CuO nanomaterials at 77 K are depicted in Fig. 4a and b, respectively. The resulting isotherm is identified as a type IV isotherm with a hysteresis loop between the p/p^0 0.8–1.0; which is the characteristic of mesoporous materials. The average pore diameter, as calculated by the Barrer–Joyner–Halenda (BJH) method was about 38.8 Å (Fig. 4b), whereas, the Brunauer–Emmett–Teller (BET) surface area of the sample was found to be about 66.63 m^2/g.

3.4. Field emission scanning electron microscopy

The surface morphology of the as-deposited CuO was studied using FESEM and is shown in Fig. 5, from which a network like frame work formed by the inter linkage of the cubic shaped CuO grains of the material is evident. On a closer look, the finer pores are also observable in the material. The average grain diameter, as determined from Fig. 5 is about 50 nm, which is to some extent higher than the value of the crystallite diameter (~20 nm) as obtain from XRD pattern analysis, which is obvious, since, the crystallites coalesce together to form grains with larger size to lower the Gibb's free energy. Fig. 5 also reveals that the grains are not highly homogeneous in shape and size, which is also quite normal when the grains coalesce together to form a network like structure like what we have obtained here.

3.5. Optical analyses

3.5.1. UV–vis studies

UV–vis absorption spectroscopy is one of the most important methods to reveal the energy structures and optical properties of semiconducting materials. Fig. 6 shows the absorption spectrum of the as-deposited CuO thin film, which shows an onset of absorption at about 425 nm, corresponds to the band gap energy (E_g) of ~2.9 eV. Compared with the reported value of E_g for bulk CuO ($E_g=1.2$ eV) [15], a blue-shift in band gap energy by an amount of 1.7 eV is evident here, which is due to the quantum confinement effect exerted by the nanosize crystals.

3.5.2. Photoluminescence studies

Fig. 7 shows the room temperature photoluminescent spectrum of CuO thin film. The excitation energy wavelength (λ_{exc}) was 325 nm, which was originated from a Xe-arc lamp. A dominant sharp emission peak around 406 nm was observed in the blue region. The blue-shift behavior of the peak position, in

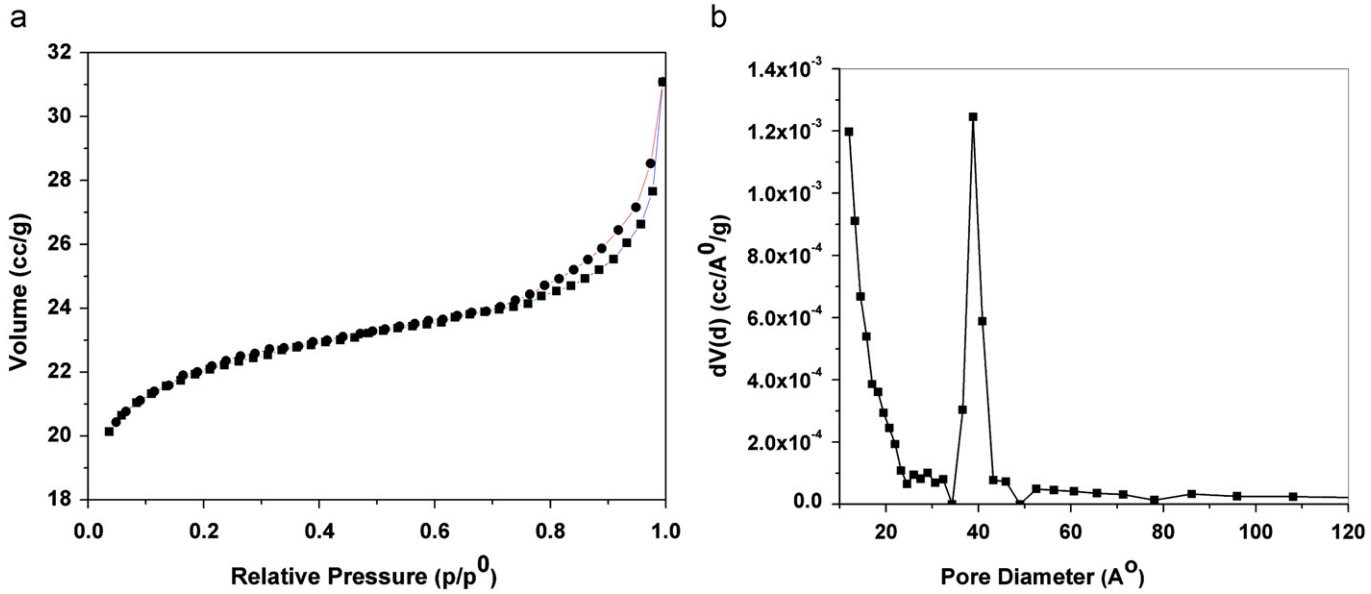

Fig. 4. (a) N_2 adsorption–desorption isotherms for powder CuO and (b) pore size distribution curve.

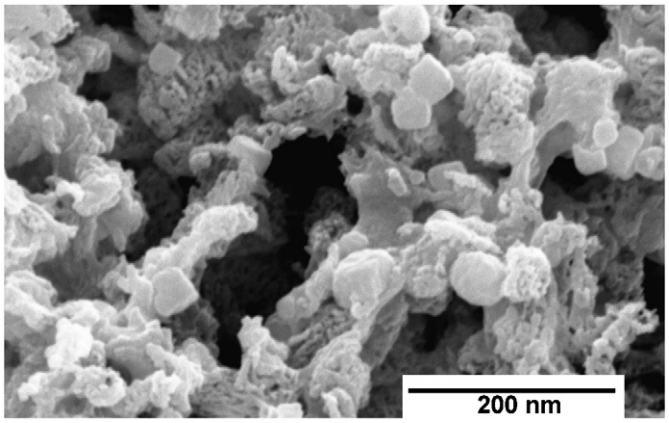

Fig. 5. FESEM image of CuO thin film.

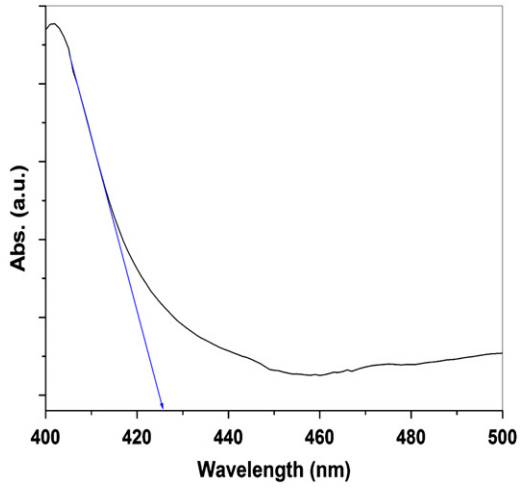

Fig. 6. UV–vis absorption spectrum of the CuO thin film.

comparison with that of the bulk CuO was also evident from this PL emission spectrum and tallies well with the findings from UV–vis analysis. This blue-shift was attributed due to the

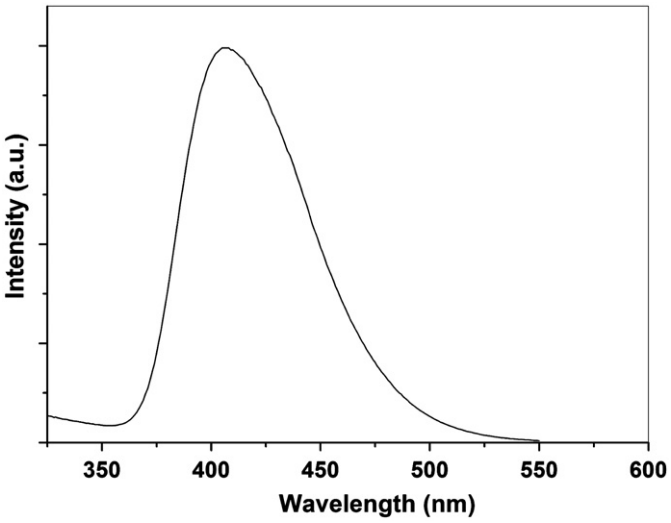

Fig. 7. PL spectrum for the CuO thin film.

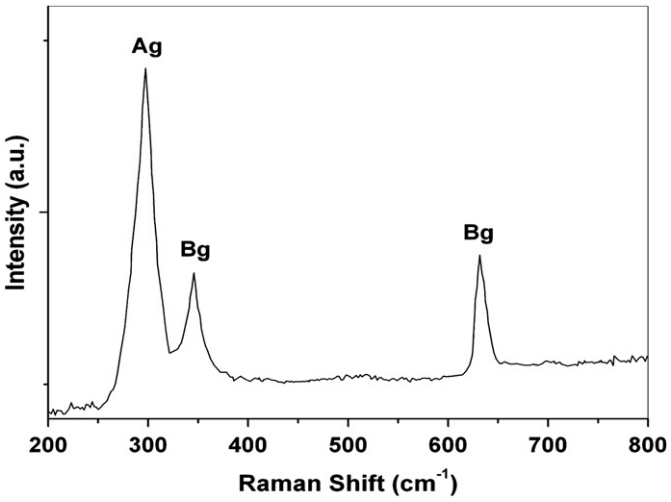

Fig. 8. Raman spectrum of the as-prepared CuO sample.

Table 1
Results of Hall measurement.

Applied magnetic field (T)	Bulk concentration (/cm^3)	Mobility (cm^2/V s)	Hall coefficient	Resistivity (Ω cm)	Magnetoresistance (Ω)
0.37	2.83×10^{13}	1.65×10^{2}	2.21×10^{5}	1.34×10^{3}	5.16×10^{5}

enhancement of the quantum confinement effect resulting from the decrease in the dimensional structure and the size of the nanoparticles.

3.5.3. Raman studies

Fig. 8 shows the room temperature Raman spectrum of CuO nanostructures. CuO belongs to the C_{2h}^6 space group with two molecules per primitive cell. One can find the zone center Raman active normal modes Γ_{RA}=4Au+5Bu+Ag+2Bg. There are three acoustic modes (Au+2Bu), six infrared active modes (3Au+3Bg), and three Raman active modes (Ag+2Bg). Three Raman active optical phonons have been identified and they are comparable to those were reported earlier in the literature by other groups, who used different technique to prepare CuO nanoparticles [16]. The Raman analysis of the CuO sample confirms the three known bands at 297, 345 and 631 cm^{-1}, corresponds to the Ag (296 cm^{-1}), Bg$^{(1)}$ (346 cm^{-1}), and Bg$^{(2)}$ (631 cm^{-1}) which is in good agreement with the previously reported data [17]. No Cu_2O modes [18] were found to be present in the CuO nanostructures prepared by us. Significant peak intensity indicates high crystalline nature of the deposited sample.

3.6. Hall measurements

To carry out the Hall measurement, CuO films with 1 cm × 1 cm area were deposited on glass substrates, following the method stated earlier. The thickness of the films were measured gravimetrically, and was found to be about 0.4 μm. Contacts was made using gold coated clips on the surface of the film by spring action and the distance between two contact points was 0.5 cm. Measurement was carried out under the magnetic field (B) of 0.37 T. The results are summarized in Table 1. The positive sign of Hall coefficient indicates that the deposited film is of p-type in nature with carrier concentration in the order of 10^{13} Ω cm.

4. Conclusions

Mesoporous CuO was prepared using a simple and convenient single precursor decomposition route. Characterizations showed that the CuO obtained from this precursor was composed of cubic shape nanoparticles of about 50 nm in diameter. BET analysis shows the mesoporous nature with surface area of 66.63 m^2/g. The quantum confinement effect exerted by such nanocrystals found to bring a significant blue-shift in the band to band transition energy of the deposited materials. A dominant emission peak in the blue region of the PL spectrum for CuO nanoparticles is observed. p-Type conduction nature of the material was established from the Hall effect measurement.

Acknowledgments

S.K. Maji is indebted to UGC, India, for his Project Fellowship [F. no. 33-31/2007 (SR)] and N. Mukherjee is indebted to CSIR, India, for his Research Associateship [Award no. 08/003(68)/2010-EMR-I]. The authors also acknowledge MHRD (India) and UGC-SAP (India) for providing instrumental facilities to the Department of Chemistry, BESUS.

References

[1] J. Switzer, J. Kothari, P. Poizot, S. Nakanishi, E. Bohannan, Nature 425 (2003) 490.
[2] O.A. Chaltykyan, Copper-Catalytic Reactions, Consultants Bureau, New York, NY, USA, 1966.
[3] A. Chowdhuri, V. Gupta, K. Sreenivas, R. Kumar, S. Mozumdar, P. Patanjali, Appl. Phys. Lett. 884 (2004) 1180.
[4] C. Wang, X.Q. Fu, X.Y. Xue, Y.G. Wang, T.H. Wang, Nanotechnology 18 (2007) 145506.
[5] X. Gao, J. Bao, G. Pan, H. Zhu, P. Huang, F. Wu, D. Song, J. Phys. Chem. B 108 (2004) 5547.
[6] K.H. Muller, High-Tc Supper Conductors and Related Materials, vol. 86, Kluwer Academic, Dordrecht, The Netherlands, 2001.
[7] J. Chen, S. Deng, N. Xu, W. Zhang, X. Wen, S. Yang, Appl. Phys. Lett. 83 (2003) 746.
[8] S.C. Yeon, W.Y. Sung, W.J. Kim, S.M. Lee, H.Y. Lee, Y.H. Kim, J. Vac. Sci. Technol. B 24 (2006) 940.
[9] Y.W. Zhu, T. Yu, F.C. Cheong, X.J. Xu, C.T. Lim, V.B.C. Tan, J.T.L. Thong, C.H. Sow, Nanotechnology 16 (2005) 88.
[10] E. Vigil, B. González, I. Zumeta, C. Domingo, X. Domenech, J. Ayllon, Thin Solid Films 489 (2005) 50.
[11] S. Anandan, X. Wen, S. Yang, Mater. Chem. Phys. 93 (2005) 35.
[12] R.A. Zarate, F. Hevia, S. Fuentes, V.M. Fuenzalida, A. Zuniga, J. Solid State Chem. 180 (2007) 1464.
[13] K. Nakamoto, Infrared and Raman Spectra of Inorganic and Coordination Compounds, 5th ed., VCH-Wiley, New York, 1997.
[14] X. Peng, G. Cui, D. Li, T. Liu, J. Mol. Struct. 967 (2010) 54.
[15] A. Raksa, T. Gardchareon, P. Chairuangsri, N. Mangkorntong, S. Choopun, Ceram. Int. 35 (2009) 649.
[16] H.F. Goldstein, D.S. Kim, P.Y. Yu, L.C. Bourne, Phys. Rev. B 41 (1990) 7192.
[17] M.A. Dar, Q. Ahsanulhaq, Y.S. Kim, J.M. Sohn, W.B. Kim, H.S. Shin, Appl. Surf. Sci. 255 (2009) 6279.
[18] K. Reimann, K. Syassen, Phys. Rev. B 39 (1989) 11113.